Allostery in a Coarse-Grained Model of Protein Dynamics

Dengming Ming
Computer and Computational Sciences Division, Los Alamos National Laboratory, Los Alamos, New Mexico 87545, USA

Michael E. Wall
Computer and Computational Sciences and Bioscience Divisions, Los Alamos National Laboratory, Los Alamos, New Mexico 87545, USA

(Received 22 June 2005; published 2 November 2005)

We propose a criterion for optimal parameter selection in coarse-grained models of proteins and develop a refined elastic network model (ENM) of bovine trypsinogen. The unimodal density-of-states distribution of the trypsinogen ENM disagrees with the bimodal distribution obtained from an all-atom model; however, the bimodal distribution is recovered by strengthening interactions between atoms that are backbone neighbors. We use the backbone-enhanced model to analyze allosteric mechanisms of trypsinogen and find relatively strong communication between the regulatory and active sites.

DOI: 10.1103/PhysRevLett.95.198103 PACS numbers: 87.15.−v

A major challenge of molecular biology is to understand regulatory mechanisms in large protein complexes that are abundant in multicelluluar organisms. To make simulation of such complexes feasible, coarse-grained models have been developed, in which a subset of the atoms in the complex are used to simulate the large-scale motions. However, principled methods to assess the accuracy of coarse-grained models are currently lacking.

In one common coarse-graining method, an all-atom model is simplified by considering effective interactions among a subset of the atoms (e.g., just the alpha carbons). The usual criterion for model accuracy is the ability of a model to reproduce atomic mean-squared displacements (MSDs). However, MSDs are just one aspect of protein dynamics—a stricter criterion for the accuracy of a coarse-grained model is the similarity between the configurational distributions of the selected atoms in the coarse-grained and all-atom models. Such a criterion is also biologically relevant, in part because the conformational distribution is a key determinant of protein activity [1].

One useful measure of the difference between conformational distributions is the Kullback-Leibler divergence $D_{\mathbf{x}}$ (see definition below) [2,3]. Recently, an analytic expression for $D_{\mathbf{x}}$ was obtained for harmonic vibrations of a protein-ligand complex both with and without a protein-ligand interaction [3]. Here we show how an equivalent expression may be applied to refine a coarse-grained model of protein dynamics. We refine an anisotropic elastic network model (ENM) [4] of trypsinogen dynamics with respect to an all-atom model calculated using CHARMM [5]. The unimodal density-of-states distribution of the ENM disagrees with the bimodal distribution obtained from the all-atom model; however, the bimodal distribution is recovered by strengthening interactions between atoms that are backbone neighbors. Finally, the backbone-enhanced elastic network model (BENM) is used to analyze allosteric mechanisms of trypsinogen.

Let $P(\mathbf{x})$ be the probability distribution of the $3N$ atomic coordinates $\mathbf{x} = (x_1, y_1, z_1, \ldots, x_N, y_N, z_N)$ of a molecular model in the harmonic approximation. Let $\mathbf{x} = (\mathbf{x}_1, \mathbf{x}_2)$, where $\mathbf{x}_1$ is the $3N_1$ coordinates of a subset of atoms of interest, and $\mathbf{x}_2$ is the $3N_2$ coordinates of the remaining atoms. We are interested in calculating the marginal distribution $P(\mathbf{x}_1)$:

$$P(\mathbf{x}_1) = \int d^{3N_2}\mathbf{x}_2 P(\mathbf{x}_1, \mathbf{x}_2). \quad (1)$$

Consider a harmonic approximation to the potential energy function $U(\mathbf{x} + \mathbf{x}_0)$, where $\mathbf{x}$ is the deviation from an equilibrium conformation $\mathbf{x}_0$:

$$U(\mathbf{x} + \mathbf{x}_0) \approx U(\mathbf{x}_0) + \tfrac{1}{2}\mathbf{x}^\dagger \mathbf{H} \mathbf{x}. \quad (2)$$

The matrix $\mathbf{H}$ is the Hessian of U evaluated at $\mathbf{x}_0$: $H_{ij}|_{\mathbf{x}_0} = \partial^2 U/\partial x_i \partial x_j|_{\mathbf{x}_0}$. We assume a Boltzmann distribution for $P(\mathbf{x})$ and ignore solvent and pressure effects:

$$\begin{aligned} P(\mathbf{x}) &= Z^{-1} e^{-\mathbf{x}^\dagger \mathbf{H} \mathbf{x}/2k_BT} \\ &= (2\pi k_B T)^{-3N/2} e^{-|\Omega \mathbf{V}^\dagger \mathbf{x}|^2/2k_BT} {\prod_{i=1}^{3N}}' \omega_i, \end{aligned} \quad (3)$$

where Z is the partition function, k_B is Boltzmann's constant, T is the temperature, the elements of the matrix $|\Omega|^2 = \mathrm{diag}(\omega_1^2, \ldots, \omega_{3N}^2)$ are the eigenvalues of $\mathbf{H}$, and the columns of the matrix $\mathbf{V}$ are the eigenvectors of $\mathbf{H}$. Here and elsewhere, products and summations are carried out over nonzero modes. Define the submatrices $\mathbf{H}_1$, $\mathbf{H}_2$, and $\mathbf{G}$ as follows:

$$\mathbf{H}\mathbf{x} = \begin{pmatrix} \mathbf{H}_1 & \mathbf{G} \\ \mathbf{G}^\dagger & \mathbf{H}_2 \end{pmatrix} \begin{pmatrix} \mathbf{x}_1 \\ \mathbf{x}_2 \end{pmatrix} = \begin{pmatrix} \mathbf{H}_1\mathbf{x}_1 & + & \mathbf{G}\mathbf{x}_2 \\ \mathbf{G}^\dagger\mathbf{x}_1 & + & \mathbf{H}_2\mathbf{x}_2 \end{pmatrix}. \quad (4)$$

$\mathbf{H}_1$ couples coordinates from $\mathbf{x}_1$; $\mathbf{H}_2$ couples coordinates from $\mathbf{x}_2$; and $\mathbf{G}$ couples coordinates between $\mathbf{x}_1$ and $\mathbf{x}_2$. In Eq. (3), $|\Omega \mathbf{V}^\dagger \mathbf{x}|^2$ now can be expressed as

$$|\Omega \mathbf{V}^\dagger \mathbf{x}|^2 = |\bar{\Omega} \bar{\mathbf{V}}^\dagger \mathbf{x}_1|^2 + |\Lambda \mathbf{U}^\dagger \mathbf{x}_2 + \Lambda^{-1} \mathbf{U}^\dagger \mathbf{G}^\dagger \mathbf{x}_1|^2, \quad (5)$$

where the diagonal elements of the matrix $|\Lambda|^2 = \mathrm{diag}(\lambda_1^2, \ldots, \lambda_{3N_1}^2)$ and the columns of the matrix $\mathbf{U}$ are the eigenvalues and eigenvectors of $\mathbf{H}_2$, and the diagonal elements of the matrix $|\bar{\Omega}|^2 = \mathrm{diag}(\bar{\omega}_1^2, \ldots, \bar{\omega}_{3N_1}^2)$ and the columns of the matrix $\bar{\mathbf{V}}$ are the eigenvalues and eigenvectors of a matrix $\bar{\mathbf{H}}$ defined as

$$\bar{\mathbf{H}} = \mathbf{H}_1 - \mathbf{G}\mathbf{H}_2^{-1}\mathbf{G}^\dagger = \bar{\mathbf{V}}|\bar{\Omega}|^2\bar{\mathbf{V}}^\dagger. \quad (6)$$

Equation (6) is equivalent to an equation independently derived to study local vibrations in the nucleotide-binding pockets of myosin and kinesin [6]. Performing the integration in Eq. (1) leads to the desired equation for $P(\mathbf{x}_1)$:

$$P(\mathbf{x}_1) = (2\pi k_B T)^{-3N_1/2} e^{-|\bar{\Omega}\bar{\mathbf{V}}^\dagger \mathbf{x}_1|^2/2k_B T} \prod_{i=1}^{3N_1}{}' \bar{\omega}_i. \quad (7)$$

Now consider the problem of optimal selection of the parameters Γ of a coarse-grained model of protein dynamics. Let $\mathbf{x}_\alpha$ be the coordinates of the N_α alpha carbons in either an all-atom model or a coarse-grained model. We define the optimal coarse-grained model as the one for which the Kullback-Leibler divergence between $P^{(\Gamma)}(\mathbf{x}_\alpha)$ and $P(\mathbf{x}_\alpha)$ is minimal, i.e., for which Γ is chosen such that

$$D_{\mathbf{x}_\alpha}^{(\Gamma)} = \int d^{3N_\alpha}\mathbf{x}_\alpha P^{(\Gamma)}(\mathbf{x}_\alpha) \ln \frac{P^{(\Gamma)}(\mathbf{x}_\alpha)}{P(\mathbf{x}_\alpha)} \quad (8)$$

is minimal. We previously calculated an analytic expression for equations like Eq. (8) when $P(\mathbf{x}_\alpha)$ and $P^{(\Gamma)}(\mathbf{x}_\alpha)$ are both governed by harmonic vibrations [3]:

$$D_{\mathbf{x}_\alpha}^{(\Gamma)} = \sum_{i=1}^{3N_\alpha}{}' \Bigg(\ln \frac{\omega_i^{(\Gamma)}}{\bar{\omega}_i} + \frac{1}{2k_B T}\bar{\omega}_i^2 |\bar{\mathbf{v}}_i^\dagger \Delta\mathbf{x}_{\alpha,0}|^2 + \frac{1}{2}\sum_{j=1}^{3N_\alpha}{}' \frac{\bar{\omega}_j^2}{\omega_i^{(\Gamma)2}} |\mathbf{v}_i^{(\Gamma)\dagger}\bar{\mathbf{v}}_j|^2 - \frac{1}{2} \Bigg). \quad (9)$$

In Eq. (9), $\omega_i^{(\Gamma)2}$ and $\mathbf{v}_i^{(\Gamma)}$ are the eigenvalue and eigenvector of mode i of the coarse-grained model, $\bar{\omega}_i^2$ and $\bar{\mathbf{v}}_i$ are the ith eigenvalue and eigenvector of the matrix $\bar{\mathbf{H}}$ calculated for the alpha-carbon atoms of the all-atom model [Eq. (6)], and $\Delta\mathbf{x}_{\alpha,0} = \mathbf{x}_{\alpha,0}^{(\Gamma)} - \mathbf{x}_{\alpha,0}$ is the difference between the equilibrium coordinates of the coarse-grained and all-atom models.

In the ENM [4], interacting alpha-carbon atoms are connected by springs aligned with the direction of atomic separation. Following the Tirion model of harmonic vibrations [7], each spring has the same force constant γ. For a given interaction network, the eigenvectors $\mathbf{v}_i^{(\Gamma)}$ are independent of γ, and each eigenvalue $\omega_i^{(\Gamma)2}$ is proportional to γ. The value of γ at which $D_{\mathbf{x}_\alpha}^{(\Gamma)}$ is minimal may be calculated using Eq. (9):

$$\gamma = \frac{1}{3N_\alpha}\sum_{i=1}^{3N_\alpha}{}' \sum_{j=1}^{3N_\alpha}{}' \frac{\bar{\omega}_j^2}{a_i^2} |\mathbf{v}_i^{(\Gamma)\dagger}\bar{\mathbf{v}}_j|^2. \quad (10)$$

Because the eigenvalues $\omega_i^{(\Gamma)2}$ are proportional to γ, the constants $a_i^2 = \omega_i^{(\Gamma)2}/\gamma$ are independent of γ. The third and fourth terms of Eq. (9) cancel when γ assumes the value given by Eq. (10).

The interaction network in an elastic network model is generated by connecting pairs of atoms separated by a distance less than or equal to a cutoff distance r_c. To optimize the model, the value of r_c for which $D_{\mathbf{x}_\alpha}^{(\Gamma)}$ is minimal is numerically estimated, using γ from Eq. (10).

As a test case, we developed a coarse-grained model of trypsinogen residues 7-229 from an all-atom model [8]. CHARMM was used for all-atom simulations using the CHARMM22 force field with default parameter values. HBUILD was used to add hydrogens, and the energy was initially minimized using 2000 steps of the adopted basis Newton-Raphson method, gradually reducing the weight of a harmonic restraint to the crystal-structure coordinates. The final minimized structure was obtained through vacuum minimization until a gradient of 10^{-7} kcal/mol Å was achieved, and the Hessian $\mathbf{H}$ was calculated in CHARMM. The coordinates of the ENM were taken from the alpha-carbon atoms of the minimized all-atom model.

The alpha-carbon vibrations of the all-atom model were calculated by diagonalizing $\bar{\mathbf{H}}$ from Eq. (6). Interestingly, the density-of-states distribution is bimodal (Fig. 1) with $2/3$ of the frequencies in the low-frequency spectrum and $1/3$ of the frequencies in the high-frequency spectrum. Calculation of the density-of-states distribution from other globular proteins yields bimodal patterns with a similar 2:1 ratio between the numbers of low- and high-frequency modes (unpublished results).

The best ENM of trypsinogen was obtained using a cutoff distance r_c of approximately 7.75 Å, for which the optimal value of γ is 53.4 kcal/mol Å^2, yielding a value of $D_{\mathbf{x}_\alpha}^{(\Gamma)} = 312.9$. The density-of-states distribution for the ENM is unimodal, unlike that for the all-atom model (Fig. 1).

Although the ENM treats all alpha-carbon pairs equally, the distribution of distances between successive alpha carbons along the protein backbone is known to be tightly centered about 3.8 Å. In addition, two of the six alpha carbons nearest to a typical alpha carbon are backbone neighbors, which might explain why $1/3$ of the CHARMM-derived modes have significantly higher frequencies than the others. We therefore wondered whether the ENM might be improved by enhancing interactions between backbone neighbors.

A more accurate coarse-grained model is obtained by using a force constant enhanced by a factor of ϵ for interactions between alpha carbons that are neighbors on the backbone. Minimization of $D_{\mathbf{x}_\alpha}^{(\Gamma)}$ for such a backbone-enhanced elastic network model with respect to ϵ and r_c subject to Eq. (10) yields a model with $\epsilon = 42$, $r_c = 10.5$ Å, and $\gamma = 4.26$ kcal/mol Å^2, resulting in a much lower value $D_{\mathbf{x}_\alpha}^{(\Gamma)} = 102.3$. The density-of-states distribution for this model agrees quite well with that of the all-

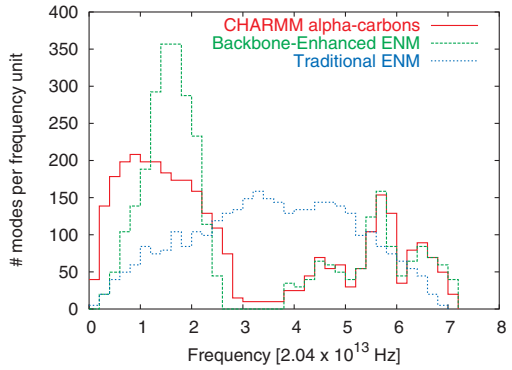

FIG. 1 (color). Density-of-states distribution for all-atom and elastic network models of trypsinogen. Frequency units are $(\text{kcal/mol Å}^2 m_p)^{1/2} = 2.04 \times 10^{13}$ Hz, where m_p is the proton mass. Densities were estimated by counting the number of modes in bins of width 0.2 and normalizing the integral to 663, which is the total number of nonzero modes.

atom model (Fig. 1), especially considering that the model is optimized with respect to $D_{\mathbf{x}_\alpha}^{(\Gamma)}$, which does not directly involve the density-of-states distribution. The agreement is especially good for the high-frequency modes, suggesting that a uniform force constant is a reasonable approximation for interactions between alpha carbons that are backbone neighbors. Furthermore, the overlap $\sum_{i=1}^{N}\sum_{j=1}^{N}|\mathbf{v}_i^{(\Gamma)\dagger}\bar{\mathbf{v}}_j|^2/N$ for the 223 highest-frequency modes is 0.99, indicating that the spaces of the high-frequency eigenvectors are nearly identical between the BENM and all-atom models.

Both the BENM and the ENM yield patterns of alpha-carbon MSDs that are similar to that of the all-atom model (Fig. 2). Because there are fewer low-frequency BENM modes than low-frequency CHARMM modes (Fig. 1), the BENM MSDs are consistently smaller than the CHARMM MSDs; however, the BENM MSDs may be improved by selecting $\gamma = 1.2$ kcal/mol Å^2 (Fig. 2). These improved MSDs come at the cost of a higher value of $D_{\mathbf{x}_\alpha}^{(\Gamma)} = 528.4$, and a change in the frequency scale by a factor $(1.2/4.3)^{1/2} = 0.53$, resulting in a poor model of the density-of-states distribution. The ENM with parameters that minimize $D_{\mathbf{x}_\alpha}^{(\Gamma)}$ exhibits poor MSDs (not shown); however, an ENM with $r_c = 15.4$ Å and $\gamma = 0.4$ kcal/mol Å^2 yields MSDs that agree well with those of the CHARMM model (Fig. 2). In agreement with previous results using the ENM [4], we confirmed that the parameters of both the ENM and BENM may be adjusted to yield a reasonable model of crystallographic MSDs (not shown).

Next consider the problem of quantifying allosteric effects in proteins [3]. In allosteric regulation, molecular interactions cause changes in protein activity through changes in protein conformation. Although the importance of considering continuous conformational distributions in understanding allosteric effects was recognized by Weber [9], theories of allosteric regulation that consider continuous conformational distributions have been lacking. We began to develop such a theory by defining the allosteric potential as the Kullback-Leibler divergence $\bar{D}_{\mathbf{x}}$ between protein conformational distributions before and after ligand binding and by calculating a related quantity using changes in the conformational distribution of the full protein-ligand complex [3]. Here we use the expression for the marginal distribution in Eq. (7) to calculate an equation for the true allosteric potential in the harmonic approximation.

Let $\mathbf{x}_p$ be the protein coordinates selected from the coordinates $\mathbf{x}$ of a protein-ligand complex. $P'(\mathbf{x}_p)$ and $P(\mathbf{x}_p)$ are the protein conformational distributions with and without a ligand interaction, respectively. Equation (7) enables $P'(\mathbf{x}_p)$ to be calculated from the full conformational distribution $P'(\mathbf{x})$ of the protein-ligand complex. The equation for the allosteric potential in the harmonic approximation follows from Ref. [3]:

$$\bar{D}_{\mathbf{x}} = \sum_{i=1}^{3N_p\prime}\left(\ln\frac{\bar{\omega}_i'}{\omega_i} + \frac{1}{2k_BT}\omega_i^2|\mathbf{v}_i^\dagger\Delta\mathbf{x}_{p,0}|^2 + \frac{1}{2}\sum_{j=1}^{3N_p\prime}\frac{\omega_j^2}{\bar{\omega}_i'^2}|\bar{\mathbf{v}}_i'^\dagger\mathbf{v}_j|^2 - \frac{1}{2}\right). \quad (11)$$

In Eq. (11), $\bar{\omega}_i'^2$ and $\bar{\mathbf{v}}_i'$ are the ith eigenvalue and eigenvector of the matrix $\bar{\mathbf{H}}$ calculated for the protein atoms of the protein-ligand complex, ω_i^2 and $\mathbf{v}_i$ are the eigenvalue and eigenvector of mode i of the apoprotein, and $\Delta\mathbf{x}_{p,0} = \mathbf{x}'_{p,0} - \mathbf{x}_{p,0}$ is the difference between the equilibrium coordinates of the protein with and without the ligand inter-

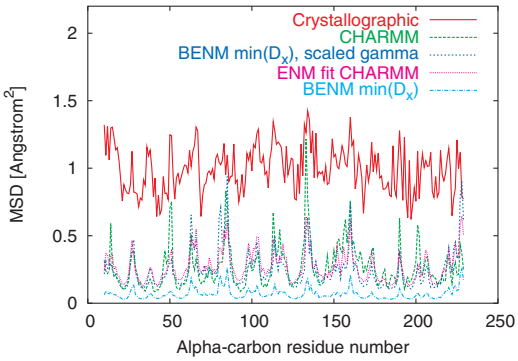

FIG. 2 (color). Mean-squared displacements of alpha-carbon positions for trypsinogen residues 10–229 obtained from normal-modes simulations using CHARMM (dashed green line), a BENM with parameters that minimize $D_{\mathbf{x}_\alpha}$ with respect to CHARMM (dotted blue line), the same BENM but with γ adjusted to better agree with CHARMM MSDs (fine-dotted magenta line), and an ENM with parameters adjusted to agree with CHARMM MSDs (dashed-dotted cyan line). Values were calculated at $T = 300$ K using the equipartition theorem. Harmonic vibrations at thermal equilibrium are known to inadequately model crystallographic MSDs, which include other sources of disorder (solid red line) [13].

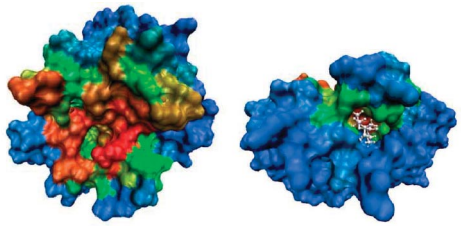

FIG. 3 (color). Visualization of local sites on the surface of trypsinogen that exhibit a large change in the conformational distribution upon binding BPTI. Values of $\bar{D}_{\mathbf{x}}$ are mapped to a logarithmic temperature scale, with red coloring indicating large values. Changes are large both in the BPTI-binding site (left) and in the active site (right). There is a 90° rotation about the x axis between the left and the right panels.

action. The term $\sum_{i=1}^{3N_p\prime} \ln\bar{\omega}_i'/\omega_i$ is proportional to the change in configurational entropy of the protein upon releasing the ligand, and $\sum_{i=1}^{3N_p\prime} \omega_i^2 |\mathbf{v}_i^\dagger \Delta\mathbf{x}_{p,0}|^2/2k_BT$ is proportional to the potential energy required to deform the apoprotein into its equilibrium conformation in the complex.

We used Eq. (11) to calculate changes in the configurational distribution of local regions of trypsinogen upon binding bovine pancreatic trypsinogen inhibitor (BPTI). Alpha-carbon coordinates were obtained from a crystal structure of the complex [8] and were used to construct BENMs of trypsinogen with and without BPTI. Both models used $r_c = 10.5$ Å, $\gamma = 4.26$ kcal/mol Å^2, and $\epsilon = 42$.

Local changes in the conformational distribution of trypsinogen were analyzed by considering changes in the neighborhood of each alpha-carbon atom. A neighborhood was defined by selecting the atom of interest plus its five nearest neighbors, and the matrix $\bar{\mathbf{H}}$ was calculated for these six atoms in the models both with (yielding $\bar{\mathbf{H}}'$) and without (yielding $\bar{\mathbf{H}}$) the BPTI interaction. A local value of $\bar{D}_{\mathbf{x}}$ was obtained using the eigenvalues and eigenvectors of $\bar{\mathbf{H}}'$ and $\bar{\mathbf{H}}$ in a suitably modified version of Eq. (11).

Not surprisingly, we found that the local values of $\bar{D}_{\mathbf{x}}$ were relatively large in the neighborhood of the BPTI-binding site (Fig. 3, left panel). Values of $\bar{D}_{\mathbf{x}}$ elsewhere on the surface were smaller, with one interesting exception: Values in the active site were comparable to those in the BPTI-binding site (Fig. 3, right panel).

Considering models beyond the ENM and BENM (and even models beyond proteins), the theory presented here leads to a general prescription for modeling harmonic vibrations using coarse-grained models of materials. To optimally model the all-atom conformational distribution, always use an energy scale for interactions that eliminates the discrepancy due to differences in the eigenvectors [Eq. (10)] and select the coarse-grained model for which the entropy of the conformational distribution is the largest [first term of Eq. (9)].

Although traditional elastic network models can explain characteristics of the functions and dynamics of proteins [10], the present study shows that they provide a poor approximation to the conformational distribution calculated from all-atom models of harmonic vibrations of proteins. Model accuracy is significantly improved by using a backbone-enhanced elastic network model, which strengthens interactions between atoms that are nearby in terms of covalent linkage. Although the backbone-enhanced model appears to accurately capture the high-frequency alpha-carbon vibrations of an all-atom model, the model less accurately captures the slower, large-scale harmonic vibrations (Fig. 1).

Using calculations of the allosteric potential, communication between the regulatory and active sites of trypsinogen was observed in a purely mechanical, coarse-grained model of protein vibrations that does not consider mean conformational changes or amino-acid identities, supporting prior arguments for the possibility of allostery without a mean conformational change [11]. Because harmonic vibrations represent a small portion of the full spectrum of highly nonlinear, large-scale protein motions, it will be interesting to use more realistic calculations of free-energy landscapes [12] to more accurately model changes in protein conformational distributions.

Supported by the U.S. Department of Energy.

[1] H. Frauenfelder and P. G. Wolynes, Science **229**, 337 (1985).
[2] S. Kullback and R. Leibler, Ann. Math. Stat. **22**, 79 (1951).
[3] D. Ming and M. E. Wall, Proteins: Struct., Funct., Genet. **59**, 697 (2005).
[4] A. R. Atilgan, S. R. Durell, R. L. Jernigan, M. C. Demirel, O. Keskin, and I. Bahar, Biophys. J. **80**, 505 (2001).
[5] B. Brooks, R. Bruccoleri, B. Olafson, D. States, S. Swaminathan, and M. Karplus, J. Comput. Chem. **4**, 187 (1983).
[6] W. Zheng and B. Brooks, Biophys. J. **89**, 167 (2005).
[7] M. M. Tirion, Phys. Rev. Lett. **77**, 1905 (1996).
[8] W. Bode, J. Walter, R. Huber, H. R. Wenzel, and H. Tschesche, Eur. J. Biochem. **144**, 185 (1984).
[9] G. Weber, Biochemistry **11**, 864 (1972).
[10] L. W. Yang, X. Liu, C. J. Jursa, M. Holliman, A. J. Rader, H. A. Karimi, and I. Bahar, Bioinformatics **21**, 2978 (2005).
[11] A. Cooper and D. T. Dryden, Eur. Biophys. J. **11**, 103 (1984).
[12] A. E. Garcia and K. Y. Sanbonmatsu, Proteins: Struct., Funct., Genet. **42**, 345 (2001).
[13] N. Go, T. Noguti, and T. Nishikawa, Proc. Natl. Acad. Sci. U.S.A. **80**, 3696 (1983).